http://dx.doi.org/10.5012/bkcs.2013.34.8.2348

Electrochemical Multi-Coloration of Molybdenum Oxide Bronzes

Sang-Min Lee, Viswanathan S. Saji, and Chi-Woo Lee*

*Department of Advanced Materials Chemistry, Korea University, Sejong 339-700, Korea. *E-mail: cwlee@korea.ac.kr*
Received March 18, 2013, Accepted May 14, 2013

We report a simple electrochemical approach in fabricating multiple colored molybdenum (Mo) oxide bronzes on the surface of a Mo-quartz electrode. A three step electrochemical batch process consisting of linear sweep voltammetry and anodic oxidation followed by cathodic reduction in neutral K_2SO_4 electrolyte at different end potentials, *viz.* −0.62, −0.80 and −1.60 V (*vs.* Hg/$HgSO_4$) yielded red, blue and yellow colored bronzes. The samples produced were analyzed by XRD, EDS, and SIMS. The color variation was suggested to be associated with the cations intercalation into the oxide formed and the simultaneous structural changes that occurred during the cathodic reduction in neutral aqueous medium.

Key Words : Mo oxide bronze, Bronzes, Electrochemistry, EQCM

Introduction

Molybdenum (Mo) and its oxides have unique structural and chemical properties and are widely investigated in the areas of catalysis, sensors, capacitors, lithium-ion batteries, solar cells, photochromism and electrochromism.[1-11] The electrochromism in Mo oxides and the formation of Mo oxide bronzes have been successfully rationalized by the theory of the simultaneous ingression of cations and electrons. The MoO_6 octahedra, with sharing the edges and corners having zigzag chains and unique layers provide the open channels for the intercalation.[1,2] The injected electrons were trapped by some Mo^{6+}, forming Mo^{5+}, and the coloration was attributed to the intervalence charge-transfer transition between Mo^{6+} and the electroreduced Mo^{5+}.[8-11]

$$MoO_3 + x\,(A^+ + e^-) = A_x Mo_x^{V} Mo_{1-x}^{VI} O_3 \qquad (1)$$

where A stands for H^+, NH_4^+ or alkali, alkaline earth, or rare earth metal ion.

Previously we reviewed fundamental electrochemistry of Mo and its oxides,[8] reported the electrochemical formation of surface Mo blue[12] in acid solution and the anionic dependence of redox poperties.[13] In this work, we wish to report our findings on the electrochemical multi-coloration of surface Mo oxide bronzes electrochemically derived from Mo in neutral aqueous solutions. To the best of our knowledge this is the first report on the fabrication of red, blue, and yellow colored bronzes on Mo in aqueous solution by an electrochemical strategy. The protocol includes a batch process consisting of (1) linear sweep voltammetry (LSV-1) from −0.70 to −0.10 V, (2) chronoamperometry (CA) at −0.10 V for 60 s and (3) linear sweep voltammetry (LSV-2) from −0.10 V to different end potentials (ranging from −0.40 to −1.80 V). LSV-1 and CA were performed to make the electrode's surface active with the formation of additional oxides/hydroxides. LSV-2 was performed to reach the desired coloration. To define the electrochemical conditions of preparing optimum Mo oxide bronzes, electrochemical quartz crystal microbalance (EQCM) technique was hired as the observed changes in current and frequency are so sensitive that the effects of the minute changes in the experimental variables of potential, sweep rate, and electrolysis time on the color of the resulting Mo bronzes can be readily detected and adjusted.

Experimental

Mo quartz QCM working electrodes consisted of Mo sputtered onto Ti/crystal at 9 MHz AT-cut quartz. The electrolyte was 0.5 M K_2SO_4. Experiments were conducted at ambient laboratory conditions. A quartz crystal microbalance (QCM 922, Princeton Applied Research) combined with a potentiostat (Versastat 3, Princeton Applied Research) was employed for electrochemical studies. The counter and reference electrodes used were Pt sheet and Hg/$HgSO_4$ (Koslow Instruments, USA), respectively.

Electrochemical experiments were started after a waiting time of 5 min (open circuit potential ~ −0.69 to −0.66 V). The electrode was subjected to LSV-1 from −0.70 to −0.10 V followed by CA at −0.10 V for 60 s. The cathodic reduction was facilitated by LSV-2, where the electrode was polarized from −0.10 V to different end potentials; ranging from −0.40 to −1.80 V. LSV-1, CA and LSV-2 were performed as a batch process. The electrochemical multi-coloration reported in this work was not exactly reproducible when one of the three steps was omitted. Similar multi-coloration was observed when the solution was carefully replaced during the step of CA. The color changes were not completely reversible upon potential reversal. The scan rate used was 20 mV/s. After the experiment, the electrode was taken out and repeatedly rinsed in water and dried in flowing N_2. AR grade (Sigma Aldrich) chemicals and double distilled water was used. Experiments were also conducted in 0.5 M Li_2SO_4. Phase structure of the Mo quartz electrodes before and after the electrochemical experiments were analyzed by X-ray diffraction (XRD, Rigagu D/max-2200)

using a Cu-Kα radiation. Energy dispersive spectrometer (EDS, Bruker 410-M) was employed for the elemental analysis. EDS measurements were conducted at 5 kV. Depth profile was investigated by secondary ion mass spectroscopy (SIMS, CAMECA IMS 7f magnetic sector) with Cs^+ as primary source (10 kV, 50 nA) with 200 μm × 200 μm raster size.

Results and Discussion

Figure 1 shows the current and frequency variations during the electrochemical coloration at the three selected end potentials. The XRD of the as-formed bronzes along with the digital photographs were provided in Figure 2. There were the distinct red, blue and yellow coloration at −0.62, −0.80 and −1.60 V (end potentials), respectively. Detailed images showing the color variation were provided in Figure 3.

The frequency change indicates a decrease in mass during CA and generally an increase in mass during LSV-2. The mass variation at the initial potential ranges (−0.70 to −0.40 V) in LSV-1 was not significant whereas a continuous decrease in mass was noticed at further positive potentials greater than −0.40 V. The decrease in mass during LSV-1 and LSV-2 (> −0.40 V) and CA suggests that a certain extent of Mo was removed from the electrode's surface at the positive potentials. Such a process can be facilitated due to the comparatively inferior stability of the Mo oxides in neutral pH.[8] The increase in mass during the reduction process (LSV-2) (< −0.4 V) can be associated with the formation of a thicker oxide/hydroxide bronze layer on the electrode's surface as was evident from the SIMS analysis (*vide infra* Figure 7). The neutral pH and the corrosion products can favour the formation of a thicker hydroxide bronze layer. The increase in mass may have contributions from the cations intercalation to the oxide/hydroxide layer.

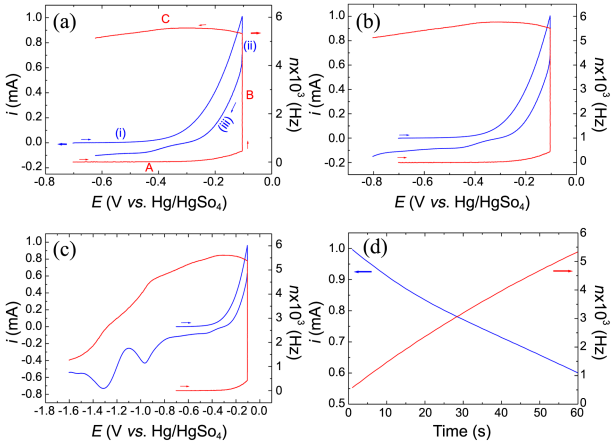

Figure 1. Current and frequency variations: (a)-(c) show plots recorded with end potentials of −0.62, −0.80 and −1.60 V, respectively (0.5 M K_2SO_4). Regions marked (i), (ii) and (iii) in the blue current line correspond to LSV-1, CA and LSV-2. The corresponding regions in the red frequency line were marked by A, B and C; (d) shows representative current and frequency changes during CA.

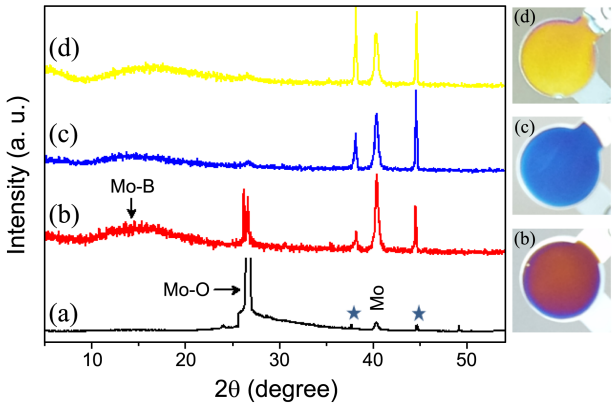

Figure 2. XRD of the samples (a) before and (b-d) after electrochemical experiment at different end potentials: (b) −0.62; (c) −0.80 and (d) −1.60 V (0.5 M K_2SO_4). Mo-B and Mo-O represent hydrated Mo oxide bronzes and MoO_3, respectively. Peaks marked by star symbol are characteristic of the Mo-quartz substrate. A magnified y axis plot is shown for (a). The corresponding digital photographs of the samples produced are also shown.

Two clear reduction peaks appeared around −1.00 and −1.30 V in LSV-2 (Figure 1(c)). The first peak can be attributed to the characteristic redox transition of Mo oxides.[8,13] The second peak may be due to a subsequent Mo oxide's reduction. Both the peaks were accompanied with a frequency decrease indicating mass gain. The mass changes for the CA step and the first and second reduction peaks were *ca.* −56 nmol Mo and +40 and +62 K nmol, respectively. The charges observed for the three processes were +490, −50, and −50 nmol e^-, respectively. The complex nature of Mo coordination chemistry ranging from simple to giant wheel-shaped clusters and of topotactic reaction chemistry of cation intercalations,[1-3] however, prohibits the detailed analysis of EQCM data. Additional EQCM data for all electrochemical experiments other than those shown in Figure 1 were also provided (Supplementary information).

When a voltage is applied to the electrochromic transition metal oxide, due to the double injection of electrons and cations into the oxide film, a rapid switching from the metallic grey to the colored form takes place with the formation of Mo oxide bronzes. In general, the bronzes can be classified as the ternary non-stoichiometric oxides of the type $A_xMo_zO_y$. Most of the reports suggested mainly three types of bronzes: blue ($A_{0.3}MoO_3$), red ($A_{0.33}MoO_3$) and purple ($A_{0.9}Mo_6O_{17}$).[1,2,6,7] The blue bronze is the widely reported one. The MoO_6 layers in the blue bronze consists of clusters of ten edge-shared octahedra linked by the corners in the [010] and [102] directions. The structure of the red bronze is similar to that of the blue bronze except that in the red bronze the unit of structure is the six edge-shared octahedra which corner share along the *b* axis and the [102] direction to form the infinite layers; the cations situated in between the layers.[1,6,7]

The bronzes formed in this study could be of the type of hydrated Mo bronzes as suggested by Schöllhorn *et al.* for the neutral aqueous electrolytes:[14-16]

$$x\,K^+ + x\,e^- + y\,H_2O + MoO_3 = [K^+(H_2O)_{y/x}]_x{\cdot}[MoO_3]^{x-} \quad (2)$$

The amorphous peak (Mo-B) (Figure 2) is assigned to the hydrated Mo oxide bronzes.

The color at −0.40 V primarily corresponds to the oxidation/reduction process occurred during CA and LSV-2 resulting in the formation of red bronzes. The reddish coloration continued down to ~ −0.62 V and thereafter it changed to the blue. In fact, the blue and red bronzes are not well defined and separated phases. The blue bronze was suggested to be the result of a limited solubility of MoO_3 in the red bronze in the case of flux melts.[17] It was reported that grinding of the polycrystalline red bronze single crystals yielded blue color and that a phase transformation occurred.[18,19] This may be the reason for the blue color formed in this study when the red colored sample was further reduced under the strong electric field applied. We think that during the reduction process, electrochemical surface structuring may take place due to the inferior stability of Mo oxides in neutral media. However, the frequency variation in EQCM showed a mass increase during the reduction. This suggests that the surface etching was not significant and that there occurred a predominant and simultaneous mass gain due to the formation of a thicker oxide/hydroxide bronze layer (see Figure 7). A stronger electrochemical surface structuring and simultaneous intercalation of cations at far negative potentials would have facilitated the yellow color formation. The yellow color may be associated with the formation of Mo bronzes of the type; $KMo_{16}O_{44}$ as was reported in the case of gadolinium Mo bronze by Galezt *et al.*[20] The oxygen content in the freely aerated electrolyte may favor such a process.

The XRD data showed a supportive evidence for the structural changes at the surface (Figure 2). The Mo quartz electrode revealed orthorhombic Mo oxides (Mo-O) peak (JCPDS: 65-2421) along with Mo (110) peak (JCPDS: 89-4896). The amorphous peak observed after the electrochemical experiments is attributed to the hydrated Mo oxide bronzes (Mo-B) (JCPDS: 47-0457). At −0.62 V, the Mo-O peak was present, however with a lowered intensity (when compared to Figure 2(a)); the peak almost disappeared at −0.82 and −1.60 V. This may be due to the formation of a porous hydroxide rich layer on the surface.[8] The increment in the intensity of the Mo (110) peak at −0.62 V may also suggest this. The two other peaks characteristic of the Mo quartz and probably related to Ti or Si were also intensified after the electrochemical experiment.

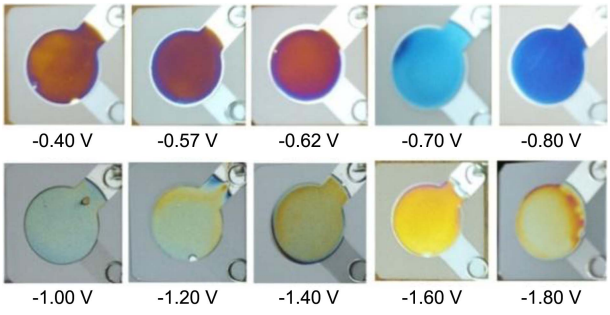

Figure 3. Digital photographs showing color variation of Mo quartz electrodes after different end potentials in 0.5 M K_2SO_4. Surface alteration from the peripheries of red colored sample revealing blue color is evident at potentials of −0.57 and −0.62 V. After the blue color formation at −0.80 V, the surface changes occurred to a higher extent at −1.00 and −1.20 V. At −1.60 V, the electrode was distinctly yellow colored.

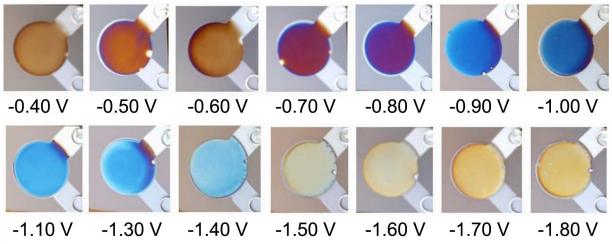

Figure 4. Digital photographs of Mo quartz electrodes after electrochemical experiment at different end potentials in 0.5 M Li_2SO_4.

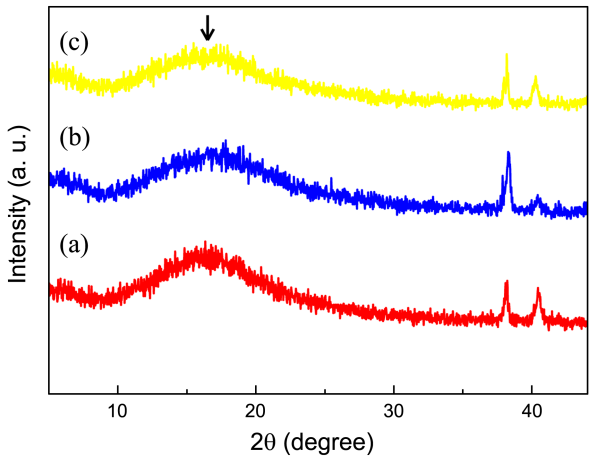

Figure 5. XRD of the samples after electrochemical experiment in 0.5 M Li_2SO_4 at different end potentials: (a) −0.70; (b) −0.90 and (c) −1.70 V. The peak corresponding to the hydrated Mo oxide bronzes is shown by an arrow mark.

Mo oxides can be electrochemically colored by incorporating various cations such as H^+, Li^+, Na^+, K^+ *etc.*[1,7] It has been shown that both Li^+ and K^+ have a similar mode of injection and attachment to the triply coordinated oxygen.[11] Our studies in Li_2SO_4 electrolyte (Figure 4) revealed a similar color variation to that of Figure 3; however the end potentials varied significantly. In Li_2SO_4, the red, blue and yellow colors appeared at −0.70, −0.90 and −1.70 V, respectively. The end potentials shifted to more negative values, suggesting that a more energy for Li^+ ingression was required to reach the desired coloration when compared to the corresponding equivalent of K^+. The XRD data (Figure 5) showed a similar variation to that of Figure 2 with the formation of amorphous hydrated Mo oxide bronzes. An EDX analysis showed supportive evidence for the formation of Mo oxide bronzes (Figure 6). The % K gradually increased on moving from red to yellow sample.

SIMS depth profiles of the samples corresponding to Figure 2 are shown in Figure 7. The K profile showed a maximum

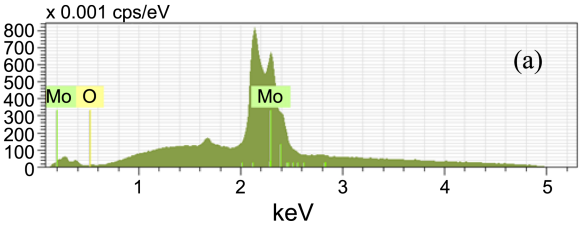

E1	AN	Series	unn. C [wt. %]	norm. C [wt. %]	Atom. C [at. %]	Error (1 Sigma) [wt. %]
Mo	42	L-series	45.95	99.93	99.57	2.29
O	8	K-series	0.03	0.07	0.43	0.05
Total :			45.99	100.00	100.00	

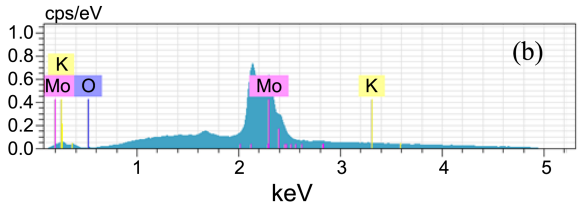

E1	AN	Series	unn. C [wt. %]	norm. C [wt. %]	Atom. C [at. %]	Error (1 Sigma) [wt. %]
K	19	L-series	15.18	29.53	50.60	3.00
Mo	42	L-series	36.22	70.42	49.19	1.81
O	8	K-series	0.03	0.05	0.21	0.04
Total :			45.99	100.00	100.00	

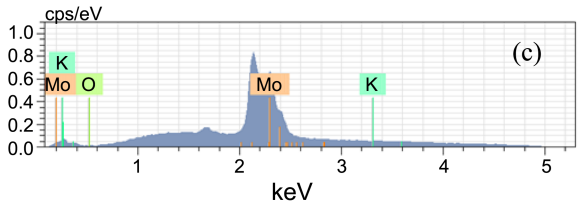

E1	AN	Series	unn. C [wt. %]	norm. C [wt. %]	Atom. C [at. %]	Error (1 Sigma) [wt. %]
K	19	L-series	13.37	30.66	51.97	2.65
Mo	42	L-series	30.23	69.30	47.88	1.52
O	8	K-series	0.02	0.04	0.15	0.04
Total :			43.62	100.00	100.00	

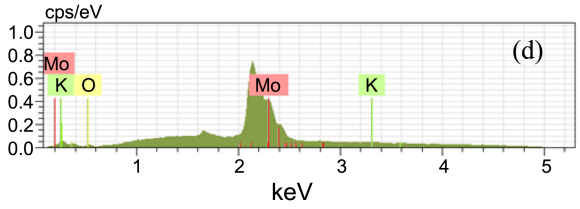

E1	AN	Series	unn. C [wt. %]	norm. C [wt. %]	Atom. C [at. %]	Error (1 Sigma) [wt. %]
K	19	L-series	14.90	38.52	59.44	2.83
Mo	42	L-series	23.55	60.87	38.28	1.19
O	8	K-series	0.23	0.61	2.28	0.09
Total :			38.68	100.00	100.00	

Figure 6. EDS analysis of (a) Mo quartz (before experiment), (b) red, (c) blue and (d) yellow colored Mo bronzes (0.5 M K_2SO_4).

at 14.50 nm in the red bronze with a subsequent drastic decrease (Figure 7(b)). The K profile in the blue bronze showed a similar variation; however, the peak maximum shifted to 20.14 nm (Figure 7(c)). In the yellow sample, the peak maximum was at 62.60 nm and a plateau region appeared (Figure 7(d)). These variations suggest that the extent

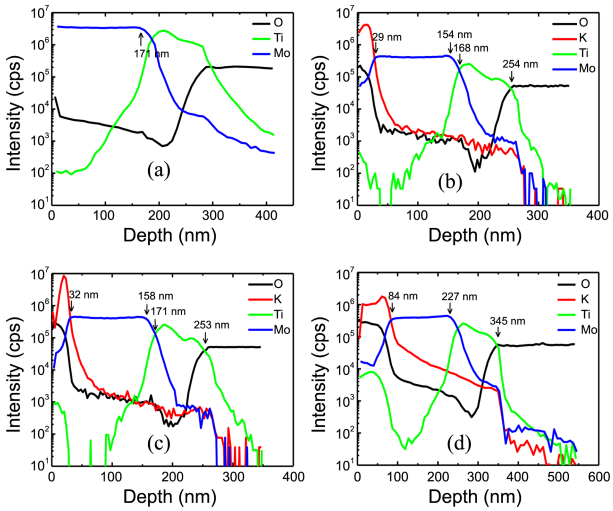

Figure 7. SIMS depth profile of Mo, K, Ti and O elements; (a) Mo quartz before experiment; (b), (c) and (d) correspond to red, blue and yellow colored bronzes formed at end potentials of –0.62, –0.80 and –1.60 V, respectively (0.5 M K_2SO_4).

of K^+ ingression/intercalation increased continuously on moving from red to yellow colored sample. On comparing the relative variation of the depth profiles of Mo and O, it can be suggested that the thickness of the oxide/hydroxide bronze layer that formed on Mo showed a gradual increase from red to yellow sample. The thicknesses of the oxide/hydroxide bronze layer in the red, blue and yellow samples were 29.10, 32.04 and 84.19 nm, respectively. This is also evident from the variation in the plateau region of the Mo profile. The plateau region appeared at ~29, 32 and 84 nm in the red, blue and yellow samples, respectively. When EQCM and SIMS profiles are compared, it can be suggested that the significant portion of the surface species formed during the reduction process remained intact on the electrode's surface. This is in accordance with the continuous weight increment observed during the LSV-2 (Figure 1). This behavior is perhaps characteristic to the Mo quartz electrode during the cathodic polarization in neutral aqueous media.

A higher starting intensity of Ti in Figure 8(d) may actually indicate an increased interference by oxygen (forming ozone, which has the same mass as that of Ti) from the increased oxide/hydroxide bronze generated during SIMS experiments or can be taken as a supportive evidence for the surface reaction (etching) progressed during electrochemical reduction (LSV-2) or both. The starting intensity of Ti increased continuously on moving from Figure 7(a) to Figure 7(d). The starting intensity of O also showed a similar trend.

The continuous increase in K^+ on moving from red to yellow sample (Figure 6 and 7) can be associated with both the end potential and the oxide/hydroxide bronze layer thickness. A higher extent of K^+ ingression at far negative potentials is as expected. The thickness factor is clearly present when the SIMS profiles of Mo and K are compared, which suggests that a greater extent of K^+ ingression in the

yellow sample occurred because of the increased thickness of the oxide/hydroxide layer. This is in accordance to our suggestion that the color change from red to blue would have originated from the marginal surface etching and the surface structural changes occurred; and not due to the variation of the extent of K^+ ingression. If the second factor (higher extent of K^+ ingression at more negative end potentials) was the determining one, the color change would have occurred from blue to red instead of red to blue. The structural change may include giant wheel-shaped clusters with nanostructured cavities.[3] More extensive K^+ in the yellow sample may support the formation of Mo bronzes of the type $KMo_{16}O_{44}$.

Conclusion

We found a simple electrochemical strategy in changing the coloration of Mo quartz electrodes in neutral aqueous electrolyte. The formation of the blue bronze from the red bronze was suggested to be due to the electrochemical surface structuring that occurred during the reduction under strong electric field applied in neutral aqueous solutions. The yellow color formed at far negative potentials may be attributed to the formation of Mo bronzes of the type $KMo_{16}O_{44}$ or to the electrochemical structural changes as described above or both. The method described herein is expected to have significant implications in the electrochemical coloring applications of Mo oxide bronzes in various sectors.

Acknowledgments. This work was financially supported by National Research Foundation of Korea (2010-0029164).

References

1. Schöllhorn, R. *Angew. Chem. Int. Ed. Engl.* **1980**, *19*, 983.
2. Greenblatt, M. *Chem. Rev.* **1988**, *88*, 31.
3. Liu, T.; Diemann, E.; Li, H.; Dress, A. W. M.; Müller, A. *Nature* **2003**, *426*, 59.
4. Ye, H.; Park, H. S.; Akhavan, V.; Goodfellow, B. W.; Panthani, M. G.; Korgel, B. A.; Bard, A. J. *J. Phys. Chem. C* **2011**, *115*, 234.
5. Park, K.-S.; Im, D.; Benayad, A.; Dylla, A.; Stevenson, K. J.; Goodenough, J. B. *Chem. Mater.* **2012**, *24*, 2673.
6. Yang, Y. A.; Cao, Y. W.; Loo, B. H.; Yao, J. N. *J. Phys. Chem. B* **1998**, *102*, 9392.
7. Colton, R. J.; Guzman, A. M.; Rabalais, J. W. *Acc. Chem. Res.* **1978**, *11*, 170.
8. Saji, V. S.; Lee, C.-W. *ChemSusChem.* **2012**, *5*, 1146.
9. Chernova, N. A.; Roppolo, M..; Dillon, A. C.; Whittingham, M. S. *J. Mater. Chem.* **2009**, *19*, 2526.
10. Dickens, P. G.; Neild, D. J. *Trans. Faraday Soc.* **1968**, *64*, 13.
11. Monk, P. M. S.; Ali, T.; Patridge, R. D. *Solid State Ionics* **1995**, *80*, 75.
12. Lee, S.-M.; Lee, C.-W. *Bull. Korean Chem. Soc.* **2012**, *33*, 1443.
13. Saji, V. S.; Lee, C.-W. *J. Electrochem. Soc.* **2013**, *160*, H54.
14. Schöllhorn, R.; Kuhlmann, R.; Besenhard, J. O. *Mater. Res. Bull.* **1976**, *11*, 83.
15. Sotani, N.; Eda, K.; Kunitoma, M. *J. Solid State Chem.* **1990**, *89*, 123.
16. Sotani, N.; Manago, T.; Suzuki, T.; Eda, K. *J. Solid State Chem.* **2001**, *159*, 87.
17. Aichele, T. *Crys. Res. Technol.* **2007**, *42*, 419.
18. Tsai, P. P.; Potenza, J. A.; Greenblatt, M. *J. Solid State Chem.* **1987**, *69*, 329.
19. Strobel, P.; Greenblatt, M. *J. Solid State Chem.* **1981**, *36*, 331.
20. Galez, Ph.; Moreau, J. M.; Marcus, J.; Escribe-Filippini, C. *Solid State Commun.* **1996**, *98*, 147.